JOURNAL OF CATALYSIS 144, 227–237 (1993)

Temperature-Programmed Desorption Studies of the Interactions of H_2, CO, and CO_2 with Cu/SiO_2

MARK J. SANDOVAL* AND ALEXIS T. BELL†

*Chemical Sciences Division, Lawrence Berkeley Laboratory, and †Department of Chemical Engineering, University of California, Berkeley, California 94720-9989

Received March 15, 1993; revised June 14, 1993

The interactions of H_2, CO, and CO_2 with a Cu/SiO_2 catalyst have been investigated using temperature-programmed desorption spectroscopy. The heats of adsorption of H_2 and CO were obtained from analysis of the experimentally observed spectra, and the activation energy for H_2 adsorption was obtained from isothermal measurements of the adsorption rate. The heat of adsorption of H_2 increases from 10.1 to 13.8 kcal/mol for $0.07 \leq \theta_H \leq 0.26$. The activation energy for H_2 adsorption is 10.5 kcal/mol, and the activation energy for H_2 desorption increases from 20.6 to 24.3 kcal/mol for $0.07 \leq \theta_H \leq 0.26$. The heat of adsorption of CO decreases with coverage from 16.4 to 12.5 kcal/mol for $0.01 \leq \theta_{CO} \leq 0.18$. The coverage by molecularly adsorbed CO_2 was below the detectable limits for adsorption temperatures above 250 K. Evidence was found, however, for a small amount of dissociatively adsorbed CO_2. The present findings are in very good agreement with recent studies on Cu single-crystal surfaces.

INTRODUCTION

The synthesis of methanol over copper-containing catalysis has been demonstrated to proceed via the reaction of adsorbed H_2 and CO and/or CO_2 on the surface of Cu crystallites (*1–4*). For this reason, knowledge of the energetics of H_2, CO, and CO_2 adsorption on Cu is critical to developing a fundamental understanding of methanol synthesis. This paper reports the results of measurements of the interactions of H_2, CO, and CO_2 with Cu/SiO_2 by temperature-programmed desorption spectroscopy.

Numerous experimental and theoretical studies have been reported concerning the adsorption of H_2 on Cu (*5–23*). In contrast to Group VIII metals, the dissociative adsorption of H_2 on Cu is an activated process due to the nearly full *3d* band of this metal. The activation energy for dissociative adsorption has been reported to be between 14.3 and 17.0 kcal/mol for low-index Cu surfaces. Atomic hydrogen once formed binds in three- and fourfold hollow sites. The heat of H_2 adsorption lies between 9 and 11 kcal/mol for various forms of unsupported Cu.

CO adsorbs molecularly on Cu surfaces without activation in linearly coordinated, on-top positions (*24–47*). Relative to Group VIII metals, the heat of adsorption of CO on Cu is low, lying between 9 and 16 kcal/mol for adsorption on bulk Cu. This characteristic is also attributed to the nearly full *3d* band of Cu.

CO_2 adsorption on Cu has been investigated on both single-crystal (*48–50*) and polycrystalline surfaces (*51*), and very recently on silica-supported Cu (*52, 53*). The coordination of CO_2 adsorbed on Cu surfaces is not generally agreed upon, although most postulated geometries have at least two of its atoms interacting with the surface (*52, 54*). The heat of adsorption for molecularly adsorbed CO_2 has been reported to lie between 6.3 and 7.5 kcal/mol for Cu(100), but values as high as 15 kcal/mol have been reported for polycrystalline Cu. For Cu/SiO_2 the heat of adsorption for molecular CO_2 has been estimated to be 6.9 kcal/mol

0021-9517/93 $5.00

(*52*). Evidence for dissociative adsorption of CO_2 on single-crystal, polycrystalline, and supported Cu has been observed (*48, 50, 51, 55*). The activation energy for the process $CO_{2,g} \rightarrow CO_g + O_s$ has been estimated to be 22 kcal/mol for Cu(100) (*50*) and 10–17 kcal/mol for Cu(110) (*56*).

EXPERIMENTAL

Catalyst Preparation and Characterization

The 8.7% Cu/SiO_2 catalyst used in this study was prepared by ion exchange following the procedure given in Ref. (*57*). One liter of 0.21 *M* $Cu(NO_3)_2$ solution was brought to pH 11 by the addition of aqueous ammonium hydroxide. Ion-exchange of $[Cu(NH_3)_4]^{2+}$ ions with the silanol groups of 30 g silica (Cab-O-Sil, Grade M-5, surface area = 200 m^2/g) took place at 298 K. The resulting slurry was dried at 383 K for 16 h, ground to 30–60 mesh size (246–600 μm), and calcined in air at 773 K for 5 h. Following calcination, the catalyst was reduced for 12 h at 623 K in H_2 flowing at 40 cm^3/min.

The weight loading of Cu was determined by X-ray fluorescence. Inductively coupled plasma emission spectroscopy (ICP) analysis of the calcined Cu/SiO_2 showed trace (<100 ppb) levels of Ca, Zn, and Fe in addition to 715 ppb Pb, 290 ppb K, and 1.1 ppm Na. ICP analysis of reduced Cu/SiO_2 which had undergone numerous CO exposures revealed an increase in the Fe and Pb levels to 340 and 1800 ppb, respectively.

The dispersion of Cu was determined following the procedure described in Ref. (*58*). A sample of freshly reduced Cu/SiO_2 is exposed for 5 min at 333 K to a flow of N_2O (20 cm^3/min) to oxidize the surface of the catalyst. At this temperature the oxidation is mild enough to assure only surface oxidation to Cu^{+1}. The amount of oxygen adsorbed, O_2, is determined by CO titration at 298 K in a 253 Torr flow of CO in He (60 cm^3/min). The amount of CO_2 evolved was measured mass spectrometrically and the number of exposed Cu atoms, Cu_s, calculated assuming the stoichiometry O_s/Cu_s = 0.5 (*58, 59*). Taking an average surface atom density for the three lowest Miller index planes of 1.47×10^{15} Cu atoms/cm^2 (*58*), the Cu dispersion is determined to be 19%.

The size and morphology of the Cu particles were determined by transmission electron microscopy (TEM) on a JEOL 200CX electron microscope operating with an accelerating voltage of 200 keV. The electron micrographs show that the Cu particles are approximately circular in shape and range in diameter from 2.0 to 5.0 nm, with an average particle diameter of 2.9 nm. Assuming a spherical geometry for the Cu particles and fcc packing, a Cu particle with a diameter of 3.0 nm should have 16% of its atoms on the surface. This value is consistent with the dispersion of 19% determined by N_2O decomposition.

Apparatus

TPD experiments were carried out in a tubular quartz reactor containing a 0.9-cm-i.d. quartz frit to support the catalyst (*60*). The reactor resides in a tubular furnace connected to a programmable temperature controller (Omega Series CN-2010), and can be heated to 1000 K. The reactor is cooled to subambient temperatures by passing liquid-nitrogen-cooled gaseous N_2 through the annular region between the microreactor and the furnace. This arrangement allows the reactor to be cooled to a minimum temperature of 110 K measured in the center of the catalyst bed.

Gases were supplied to the reactor from a gas manifold. The flow rate of each gas was controlled by either a mass flow controller (Tylan FC-280) or a needle valve and a rotometer (Fischer and Porter Model 10A3665A). CO (Matheson UHP 99.9% minimum) was purified using Oxysorb (Alltech) for O_2 removal, Ascarite (Thomas Scientific) for CO_2 removal, molecular sieve (Linde 13X) for H_2O and CO_2 removal and glass beads heated to 573 K for metal carbonyl removal. CO_2 (Matheson 4.19% CO_2/UHP He) was used directly from the cylinder without further purification. H_2 (Mathe-

son UHP, 99.999% minimum) was purified by passage through a De-Oxo catalytic hydrogen purifier (Engelhard Industries) to convert any oxygen impurity to water. The water was then removed by a molecular sieve (Linde 13X) trap immersed in liquid N_2. He (Matheson UHP, 99.999% minimum) was further purified by passage through an oxygen adsorbent (Alltech) followed by a bed of molecular sieve (Linde 13X) immersed in liquid N_2.

The desorbing gases were analyzed by an on-line quadrupole mass spectrometer (UTI Model 100C). A portion of the effluent from the reactor, or the reactor bypass, was introduced through a variable leak valve (Granville-Philips Series 203) into the vacuum chamber containing the mass spectrometer. Data from the mass spectrometer were acquired by a personal computer (Fountain PC/XT).

Procedure

A typical TPD/TPRS experiment was initiated by He purging of ~0.1 g 30/60 mesh Cu/SiO_2 at 573 K followed by evacuation to 30 mTorr, to remove any H_2O remaining after reduction of the catalyst. The temperature was then lowered to the desired adsorption temperature while still under flowing He. Adsorption of H_2, CO, or CO_2 was accomplished by flowing the adsorbate over the catalyst for 5 min at a flow rate of 20 cm^3/min. While still at the adsorption temperature, the reactor was purged with flowing He (80 cm^3/min) for 5 min, after which it was evacuated to 30 mTorr. More than one purge/pump cycle was often necessary to achieve a vacuum of 30 mTorr following the adsorption of CO at the lowest adsorption temperatures. The coadsorption experiments involved sequential doses of 5 min duration of H_2 and CO. The same purge/pump cycles were carried out after each adsorption. Subsequent to the final evacuation, a He flow of 40 cm^3/min was passed through the reactor and data acquisition was initiated. Once a steady baseline for the monitored masses was achieved, temperature programming was begun at a rate of 10 K/min.

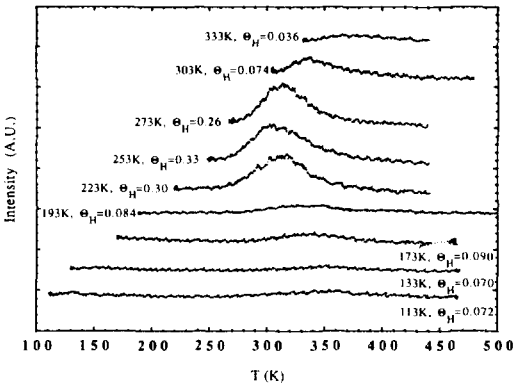

FIG. 1. TPD spectra of H_2 desorption from Cu/SiO_2. The legend indicates the initial coverage by atomic H after 5 min of exposure to 1 atm of H_2 at the specified adsorption temperature followed by evacuation.

RESULTS AND DISCUSSION

H_2 Adsorption

The TPD spectra of H_2 adsorbed on Cu/SiO_2 are shown in Fig. 1, and the uptake of H_2 as a function of adsorption temperature is given in Fig. 2. The indicated coverages are defined as the number of hydrogen atoms per surface Cu atom. Hydrogen adsorption at 113 K on SiO_2 reduced in 40 cm^3/min H_2 for 12 h at 623 K results in a small low-temperature desorption peak. The indi-

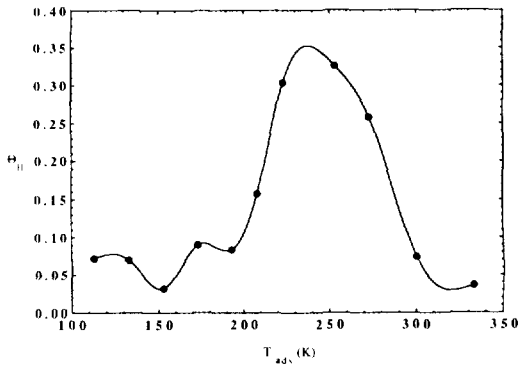

FIG. 2. Initial coverage of Cu by atomic H following 5 min of exposure to 1 atm of H_2 at the indicated adsorption temperature and subsequent evacuation.

cated coverages, θ_H, have been corrected for the small amount of H_2 adsorbed on the SiO_2.

Figure 2 shows that for a fixed adsorption time, the amount of adsorbed H_2 increases and decreases with temperature so as to produce three peaks. This pattern was obtained reproducibly and suggests that there may be as many as three adsorption states, each characterized by a different activation energy of adsorption and desorption. The origin of the two peaks observed below 200 K is unclear, but may be due to H_2 adsorption on defect sites of high coordination. The maximum uptake of H_2 is 0.33 ML at 253 K. This magnitude is somewhat smaller than the value of $\theta_H = 0.5$ observed for H_2 adsorption at 190 K on the (100), (110), and (111) surfaces of Cu (*21*).

The heat adsorption for H_2 on Cu/SiO_2 was determined by the method of desorption-rate isotherms (*61*), modified to account for the effects of equilibrium readsorption (*62*). During a TPD experiment the rates of adsorption and desorption are assumed to be equal and described by Langmuir–Hinshelwood kinetics for a mobile adsorbed layer. Neglecting spatial variations in the gas-phase concentration, the following expression for the desorption rate results:

$$\ln r_d = \ln\{Q\nu_d/m\sigma\beta\nu_a\} - q_{st}/RT + n\ln\{\theta_H/(1-\theta_H)^{p/n}\}. \quad (1)$$

Here q_{st} is the isosteric heat of adsorption, r_d is the rate of desorption, σ is the Cu metal area, m is the number of moles of Cu available for adsorption per unit area, θ_H is the number of hydrogen atoms adsorbed per surface Cu atom, Q is the volumetric flow rate of the carrier gas, p and n are the orders of adsorption and desorption, respectively, and ν_a and ν_d are the preexponential factors for adsorption and desorption, respectively.

Plots of $\ln(r_d)$ versus $\ln\{\theta_H/(1-\theta_H)^{p/n}\}$ at constant temperature were constructed by taking vertical cuts through the desorption spectra in Fig. 1. The data plotted in this fashion appear as straight lines with an average slope of 2.03, consistent with the assumption of second-order adsorption and desorption kinetics (i.e., $n = p = 2$). In the second step of the data analysis, lines of $\ln(r_d)$ versus $1/T$ at constant coverage are constructed by taking the intersection of a line of constant coverage with the isothermal plots of $\ln(r_d)$ versus $\ln[\theta_H/(1-\theta_H)]$. The slope of the lines of $\ln(r_d)$ versus $1/T$ is equal to $-q_{st}/R$.

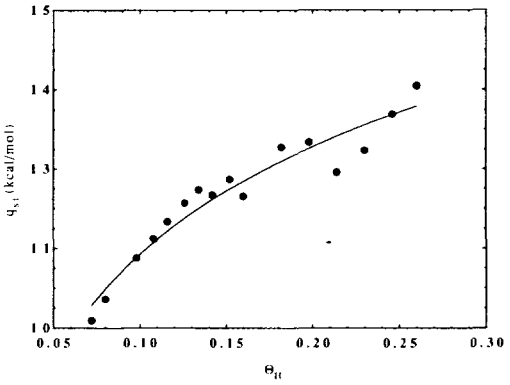

FIG. 3. Coverage dependence of the heat of adsorption of H_2 on Cu/SiO_2.

Figure 3 shows a plot of q_{st} versus θ_H. The magnitude of q_{st} rises from 10.1 kcal/mol at $\theta_H = 0.072$ to 13.8 kcal/mol at $\theta = 0.26$. As seen from Table 1, the observed range of values for q_{st} agrees well with the values reported in the literature for unsupported Cu.

The activation energy for adsorption of H_2 on Cu/SiO_2 was determined from measurements of the initial rates of adsorption. A stream of H_2 was passed over the catalyst

TABLE 1

H_2 Heats of Adsorption

Surface	q_{st} (kcal/mol)	Coverage	Ref.
Cu(311)	9.0–10.0	—	(*23*)
Cu film	13.0	Low	(*12*)
	10.0	High	(*12*)
Cu Powder	10.0	Low	(*13*)
	11.4	Low	(*14*)
	10.4	High	(*14*)
8.7% Cu/SiO_2	10.1–13.8	$0.070 \le \theta_H \le 0.26$	This study

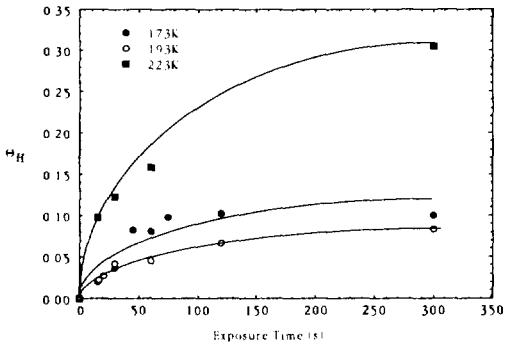

FIG. 4. Uptake of H_2 as a function of time of exposure to 1 atm H_2 at the indicated adsorption temperature and subsequent evacuation.

for a fixed period of time and the uptake measured by TPD. Temperatures and exposure times were chosen to give conditions far from equilibrium. Figure 4 shows plots of the coverage as a function of time of exposure to H_2. The rate of H_2 adsorption was determined from the initial slope of the curves. An Arrhenius form of the rate constant was assumed and the activation energy of adsorption calculated from

$$P_{ads} = \nu_a(1 - \theta_H)^2 \exp(-E_a/RT), \quad (2)$$

where P_{ads} is the probability for dissociative adsorption of H_2, ν_a is the preexponential factor, and E_a is the activation energy for adsorption. A value for ν_a of $10^{0.03\pm0.16}$ H_2 molecule adsorbed per H_2 collision with the surface was taken from the work of Campbell and Campbell (*20*) on Cu(110). Fitting Eq. (2) to the initial rates of adsorption yields activation energies for adsorption of 9.4, 10.5, and 11.5 kcal/mol for adsorption temperatures of 173, 193, and 223 K, respectively. Table 2 shows that the average value of E_a = 10.5 kcal/mol obtained from the present experiments is somewhat smaller than that previously reported for low-index planes of Cu (*5*, *20–22*) but much closer to the values of E_a measured recently for Cu(100) (*23*). We believe that the lower values of E_a measured for supported Cu crystallites may reflect the presence of high-index facets on such particles. In a recent infrared study of CO adsorbed on Cu/SiO_2, Clark *et al.* (*52*) noted that the proportions of CO adsorbed on low- and high-index planes are roughly equivalent. Consistent with this reasoning, Gregory *et al.* (*63*) have concluded on the basis of quantum chemical calculations that Cu(311) surfaces should be significantly more active for the dissociation of H_2 than Cu(100), Cu(110), or Cu(111).

TABLE 2

Activation Energy for H_2 Adsorption

Surface	E_a (kcal/mole)	Coverage	Ref.
Cu(111)	17.0	—	(*21*)
Cu(110)	14.3	$0.1 < \theta_H < 0.45$	(*20*)
	15.3	—	(*22*)
	17.0	—	(*21*)
Cu(100)	17.0	—	(*21*)
	11.4	$0.05 < \theta_H < 0.65$	(*23*)
8.7% Cu/SiO_2	9.4–11.5	—	This study

An estimate for the activation energy of desorption can be obtained from the relation $E_d = E_a + q_{st}$. Using the low coverage heat of adsorption of 10.1 kcal/mol and an activation energy of adsorption of 10.5 Kcal/mol for Cu/SiO_2, the activation energy for desorption is calculated to be 20.6 kcal/mol. Table 3 shows that this value is in very good agreement with the values reported in the literature for bulk Cu.

CO Adsorption and Desorption

The TPD spectra of CO adsorbed on Cu/SiO_2 are shown in Fig. 5, and the uptake of

TABLE 3

Activation Energy for H_2 Desorption

Surface	E_d (kcal/mol)	Coverage	Ref.
Cu(111)	20.0	$\theta_H \leq 0.2$	(*21*)
	17.0	$0.2 < \theta_H \leq 0.35$	(*21*)
Cu(110)	14.0–23.0	$0.1 \leq \theta_H \leq 0.30$	(*21*)
Cu film	20.0	Low	(*43*)
Cu ppt	20.0	—	(*30*)
1% Cu/SiO_2	20.0	—	(*30*)
8.7% Cu/SiO_2	20.6–24.3	$0.07 < \theta_H < 0.26$	This study

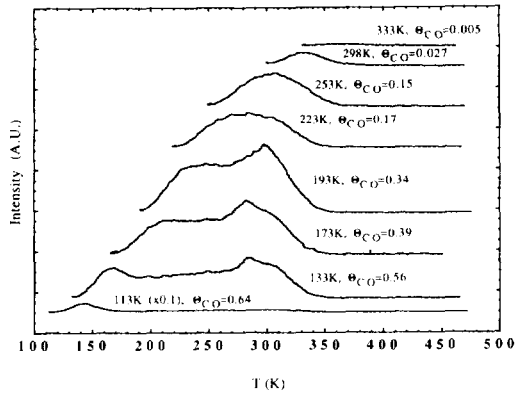

FIG. 5. TPD spectra of CO desorption from Cu/SiO_2. The legend indicates the initial coverage by CO after 5 min of exposure to 1 atm of CO at the specified adsorption temperature followed by evacuation.

CO as a function of adsorption temperature is given in Fig. 6. The indicated values of θ_{CO} are defined as the number of CO molecules adsorbed per surface Cu atom. These coverages correspond to CO desorbing from Cu only, that originating from SiO_2 having been subtracted out. The TPD spectra in Fig. 5, however, include the contribution from the SiO_2. Studies of CO adsorption on reduced SiO_2 indicate that CO occupies a physically adsorbed state below adsorption temperatures of 133 K. This weakly adsorbed CO accounts for approximately 0.25 and 0.10 of the initial desorption peaks for CO adsorbed at 113 and 133 K, respectively. The total amount of CO adsorbed on SiO_2 decreases by a factor of 10 on increasing the adsorption temperature from 113 to 133 K. The CO desorbs from SiO_2 in a single symmetric peak coincident with the initial desorption of CO from the Cu crystallites.

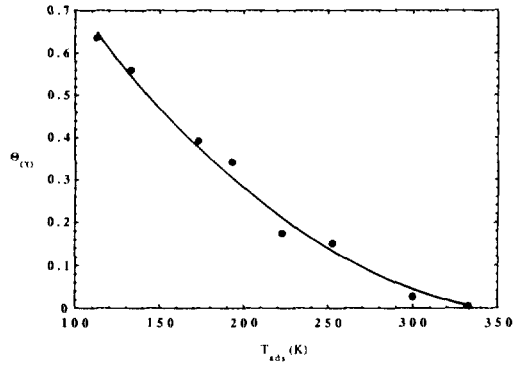

FIG. 6. Initial coverage of Cu by CO following 5 min of exposure to 1 atm of CO at the indicated adsorption temperature and subsequent evacuation.

The method of desorption rate isotherms could not be used to determine the heat of adsorption for CO on Cu/SiO_2 due to the lack of desorption spectra displaying peaks from a single distinct desorption state. Instead, the heat of adsorption was calculated from the desorption-peak maximum temperature by using the method of Scholten and Kovalinka (*64, 65*), which accounts for the effects of equilibrium readsorption. During a TPD experiment the rates of adsorption and desorption are assumed to be equal and described by Langmuir–Hinshelwood kinetics for a mobile adsorbate layer. In the absence of concentration gradients in the reactor, the heat of adsorption can be determined from

$$2 \ln T_p - \ln \beta = \Delta H_{ads}/RT_p + \ln\{(1 - \theta_p)2V_c V_m \Delta H_{ads}/(FRA^*)\}, \quad (3)$$

where ΔH_{ads} is the enthalpy of adsorption equal to $-q_{st}$, θ_p the adsorbate coverage at the desorption peak maximum, V_c the volume of the catalyst in the bed, V_m the number of moles of metal available for adsorption per unit volume catalyst, F the molar flow rate of the carrier gas, and A^* the preexponential factor of the desorption equilibrium constant (viz., $A^* = \exp(\Delta S/R)$).

It is assumed implicitly in Eq. (3) is that A^* is temperature independent. As described in detail in Ref. (65), however, the temperature dependence of the entropy may have a pronounced effect on the shape of the desorption spectrum. To account for the temperature dependence of A^* explicitly, an expression was derived using the statistical mechanical definition of the equilibrium constant, K_{eq}, for adsorption (*66*),

$$K_{eq} = K_0 T^{-r} \exp(U_{ads}/RT), \quad (4)$$

where K_0 is the temperature-independent portion of K_{eq}, U_{ads} is the differential energy of adsorption (i.e., the potential energy in the vibrational ground state which is equal to $(RT + q_{st})$), and r the value of the power-law temperature dependence of K_{eq}. The term (K_0T^{-r}) is related to A^* in Eq. (3) through the relation $1/A^* = (K_0T^{-r})$. Assuming CO adsorption on Cu obeys a Langmuir isotherm, the absence of concentration gradients in the gas phase, equilibrium readsorption and Langmuir–Hinshelwood kinetics of adsorption and desorption, an expression similar to Eq. (3) can be derived which takes into account the temperature dependence of the entropy. The final result is given by (*67*)

$$r \ln T_p - \ln \beta = U_{ads}/RT_p + \ln\{N_a \sigma m k_B (1 - \theta_p)^2 K_0 U_{ads}/Q\} + \ln\{r + U_{ads}/RT_p\}, \quad (5)$$

where Q is the volumetric carrier gas flow rate, N_a is Avogadro's number, and k_B is the Boltzmann constant. K_0 and r can be determined through evaluation of the partition functions for CO in the gas and Cu phases. Over the temperature range of interest (280–335 K), the values of r and K_0 are 7/2 and 2.19–9.66 $\times$ 10^{-6} cm^2 $K^{7/2}$ $dyne^{-1}$, respectively.

Application of Eq. (5) to the low coverage desorption spectra of Fig. 5 results in heats of adsorption of 12.5, 13.7, 15.1, and 16.5 kcal/mol for adsorption temperatures of 223, 253, 298, and 333 K, respectively. Since, as shown in Fig. 6, the coverage of CO decreases monotonically with increasing adsorption temperature, the observed increase in the heat of adsorption with increasing temperature can be attributed to the decrease in θ_{CO}. Table 4 compares these values with those for CO adsorbed at low coverages ($\theta_{CO} < 0.3$) on precipitated Cu (*29*), Cu/SiO_2 (*30, 31*), and the (100), (110), (311), and (211) planes of Cu (*26, 27, 33, 40, 41, 68, 69*). The results of the present investigation are seen to agree quite well with those reported earlier.

The maximum CO coverages obtained at 113 and 133 K are 0.64 and 0.56, respectively (see Fig. 5). These values agree closely with those reported by Pritchard (*28*) based on LEED and surface potential studies of CO adsorbed on the (100), (110), and (311) surfaces of Cu. On Cu(100) linearly adsorbed CO forms a $c(2 \times 2)$ structure at $\theta_{CO} = 0.5$ which at higher coverages undergoes a compression in the [011] direction, resulting in $\theta_{CO} = 0.58$. Upon compression, $\frac{3}{4}$ of the CO molecules remain in the linear sites and account for the observed infrared band, while $\frac{1}{4}$ relax to occupy bridge sites. IR bands corresponding to CO adsorbed in the bridge sites have not been observed. Similar work on the (110) and (311) surfaces shows that the (110) plane forms an initial $p(2 \times 1)$ structure at $\theta_{CO} = 0.5$. At higher coverages, however, CO forms compression structures which are no longer simply related to the substrate. CO adsorbed on Cu(110) at 110 K is also compressed at higher coverages to give a $c(1.3 \times 2)$ structure at $\theta_{CO} = 0.58$.

TABLE 4

Heat of Adsorption for CO

Surface	q_{st} (kcal/mol)	Coverage	Ref.
Cu(100)	16.5	$\theta_{CO} < 0.1$	(*41*)
	14.0	$0.1 \le \theta_{CO} \le 0.5$	(*41*)
	11.0	$\theta_{CO} \ge 0.5$	(*41*)
	16.0	$\theta_{CO} < 0.15$	(*26*)
	12.7	$0.15 \le \theta_{CO} \le 0.35$	(*26*)
	11.0	$\theta_{CO} \ge 0.5$	(*26*)
	14.5	Low	(*68*)
Cu(111)	10.8	$\theta_{CO} = 0.33$	(*42*)
Cu(110)	14.3	$\theta_{CO} < 0.5$	(*27*)
	12.9	$\theta_{CO} < 0.3$	(*40*)
	10.0	$\theta_{CO} \ge 0.4$	(*40*)
Cu(311)	14.3	$\theta_{CO} < 0.33$	(*33*)
Cu(211)	14.6	Low	(*69*)
Cu film	9.5–10.0	—	(*42*)
	9.0	—	(*72*)
Cu ppt	16.0	Low	(*30*)
	9.0–10	High	(*30*)
9.5% Cu/SiO_2	10.7	$\theta_{CO} < 0.1$	(*31*)
	6.0	$0.2 \le \theta_{CO} \le 0.5$	(*31*)
1% Cu/SiO2	9.0–10	High	(*30*)
8.7% Cu/SiO2	16.5–12.5	$0.01 \le \theta_{CO} \le 0.18$	This study

H_2 and CO Sequential Adsorption

TPD spectra were acquired for the desorption of H_2 from a Cu/SiO_2 catalyst fol-

lowing the sequential adsorption of H_2 and then CO. As described in the Experimental section, H_2 was adsorbed first for 5 min at a fixed temperature. The sample was then purged with He and pumped to 30 mTorr and subsequently exposed for 5 min to CO. The uptake of H_2 as a function of adsorption temperature is given in Fig. 7 for both H_2 adsorbed alone and following the sequential adsorption of H_2 and CO. The corresponding plots for CO adsorbed alone and following H_2 adsorption are shown in Fig. 8. It is evident from these figures that the adsorption of CO displaces hydrogen from the Cu surface and that the presence of hydrogen inhibits the adsorption of CO.

Sequential adsorption studies in which the order of exposure of the catalyst to CO and H_2 was reversed showed a strong influence of the adsorbate coverage with order of adsorption. Relative to CO exposure to preadsorbed H_2, exposure of the catalyst to CO followed by exposure to H_2 at 113 K resulted in a decrease in θ_H from 0.058 to 0.023 and a decrease in θ_{CO} from 0.468 to 0.350. Similarly, sequential exposure to CO followed by H_2 at 253 K resulted in a decrease in θ_H from 0.216 to 0.092 and a very small change in θ_{CO} from 0.059 to 0.070 relative to the reverse adsorption order. These data points are also shown in Figs. 7 and 8.

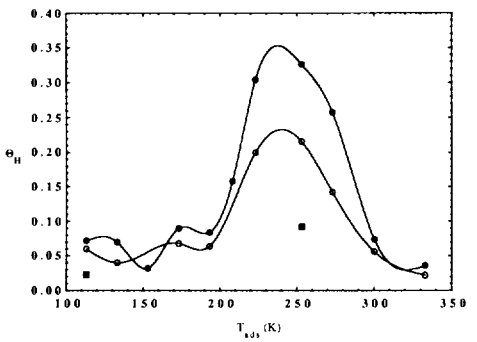

FIG. 7. Initial coverage of Cu by atomic H following 5 min of exposure to 1 atm of H_2 at the indicated adsorption temperature (●) and following the subsequent exposure to 1 atm CO (○). Also shown is the coverage of atomic H following the exposure of the catalyst to 1 atm of CO and subsequent exposure for 5 min to 1 atm of H_2 (■). Weakly held adsorbate is removed by evacuation after each gas exposure.

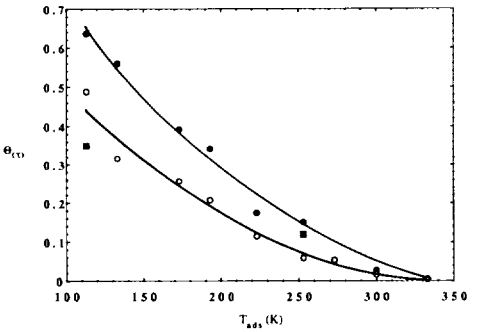

FIG. 8. Initial coverage of Cu by CO following 5 min of exposure to 1 atm of CO at the indicated adsorption temperature (●) and following the subsequent exposure to 1 atm H_2 (○). Also shown is the coverage by CO following the exposure of the catalyst to 1 atm of H_2 for 5 min and subsequent exposure to CO (■). Weakly held adsorbate is removed by evacuation after each gas exposure.

It is evident from Figs. 7 and 8 that even small amounts of preadsorbed H_2 have a significant effect on the adsorption capacity of Cu for CO, and that CO adsorption causes a moderate decrease in the amount of adsorbed H_2. Since the sum of θ_H and θ_{CO} is well under a monolayer in all cases, the effects of adsorbed CO on preadsorbed H_2 can be attributed to H-CO through-metal interactions. As interpreted by the bond-order-conservation-Morse-potential approach, such interactions result in a mutual weakening of both adsorbates (*70*). Since the heats of adsorption of H_2 and CO are comparable for Cu, the adsorption of both molecules would be expected to be affected, in contrast to what is observed for transition metals for which the heat of adsorption of CO is significantly larger than that for H_2, so that only the adsorption of H_2 is affected (*71*). The strong influence of preadsorbed CO on the adsorption of H_2 can be attributed to blockage of sites at which the dissociation of H_2 can occur. Because the uptake of H_2 in this case is small, the effect of H_2 adsorption on the quantity of adsorbed CO is small.

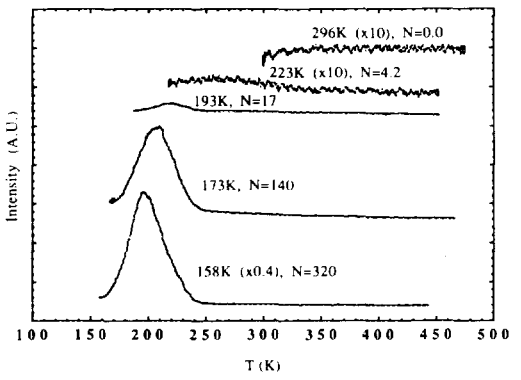

FIG. 9. TPD spectra of CO_2 desorption from Cu/SiO_2. The legend indicates the number of micromoles of CO_2 adsorbed per gram of catalyst following exposure for 5 min to 32 Torr of CO_2 at the indicated temprature.

CO_2 Adsorption and Desorption

TPD spectra of CO_2 adsorbed on freshly reduced Cu/SiO_2 are shown in Fig. 9. The adsorption temperatures and coverages are indicated adjacent to each desorption spectrum. The coverage is defined as the number of CO_2 molecules adsorbed per gram catalyst, as CO_2 readily adsorbs on both components of the catalyst (*52*). For adsorption temperatures below 193 K CO_2 desorbs immediately upon heating to give a single symmetric desorption peak at ~200 K. This peak is attributable to condensed CO_2, for which the sublimation temperature is 200 K. At higher adsorption temperatures, the amount of CO_2 adsorbed decreases dramatically, and at 296 K only a very small amount of irreversibly adsorbed CO_2 is observed. The desorption of CO was not observed for any of the conditions studied. However, reduction of the catalyst with CO following CO_2 TPD indicates surface oxygen coverages of 17%, 6.6%, and <1% for CO_2 adsorption at 173, 223, and 296 K, respectively.

The results reported here closely agree with those reported recently by Clarke *et al.* (*52*). By *in situ* infrared spectroscopy, these authors observed that exposure of a Cu/SiO_2 catalyst to 150 Torr CO_2 at 303 K resulted in the adsorption of 0.05 of a monolayer of CO_2 on the surface of the Cu particles. Purging the gas phase reduced the CO_2 coverage to 0.006. The heat of adsorption of CO_2 was estimated to be 6.9 kcal/mol. During CO_2 exposure a portion of the adsorbed CO_2 was found to undergo dissociation to CO_s and O_s. The coverage of adsorbed CO reached a maximum coverage of about 0.001 after about 3 min of CO_2 exposure, and then slowly decreased. In the light of these results, it is not surprising that little evidence was seen in the present study for either adsorbed CO_2 or the products of CO_2 dissociation after exposure of the catalyst to CO_2 at 296 K.

CONCLUSIONS

The adsorption of H_2 on Cu/SiO_2 is an activated process. Studies of H_2 uptake versus temperature suggest that there may be as many as three adsorption states and that the maximum coverage of adsorbed H is 0.33. The activation energy for adsorption is estimated to be 10.5 kcal/mol. The value is lower than that observed for low-index facets of Cu, suggesting that H_2 adsorption may occur preferentially on high-index facets. The heat of adsorption of H_2 increases with increasing coverage from 10.1 to 13.8 kcal/mol for $0.07 \leq \theta_H \leq 0.26$ and over the same range of coverages the activation energy for desorption increases from 20.6 to 24.3 kcal/mol. The observed values of the heat of adsorption and the activation energy for desorption are in agreement with measurements of these parameters for low-index facets of Cu single crystals and polycrystalline Cu.

The adsorption of CO on Cu/SiO_2 is not activated, and, hence, the uptake of CO decreases with increasing temperature. The heat of adsorption of CO is found to decrease with increasing CO coverage from 16.4 to 12.5 kcal/mol for $0.01 \leq \theta_{CO} \leq 0.18$. These values, together with the observation of maximum CO coverages of 0.64 and 0.56 at 113 and 133 K, respectively, are in good agreement with measurements made for low-index facets of Cu.

Sequential adsorption of H_2 and CO indicates that the uptake of each gas is strongly influenced by the sequence of gas adsorption. A mutual weakening of the strength of adsorbate interaction with Cu is observed, which is attributed to H–CO through-metal interactions.

Multilayer adsorption of CO_2 is observed for adsorption temperatures below 193 K, and the amount of irreversibly adsorbed CO_2 decreases very rapidly as the temperature increases to 296 K. While the amounts of CO_2 adsorbed at near ambient temperatures were below the detectable limits, evidence was found for dissociative CO_2 adsorption. These findings are consistent with recent infrared studies indicating that CO_2 interacts very weakly with Cu/SiO_2.

REFERENCES

1. Chinchen, G. C., Spencer, M. S., Waugh, K. C., and Whan, D. A., *J. Chem. Soc. Faraday Trans. 1* **83,** 2193 (1987).
2. Chinchen, G. C., Denny, P. J., Parker, D. G., Spencer, M. S., and Whan, D. A., *Appl. Catal.* **30,** 333 (1987).
3. Fleisch, T. H., and Mieville, R. L., *J. Catal.* **90,** 165 (1984).
4. Bridgewater, A. J., Wainwright, M. S., Young, D. J., Orchard, J. P., *Appl. Catal.* **7,** 369 (1988).
5. Harris, J., *Surg. Sci.* **221,** 335 (1989).
6. Harris, J., and Andersson, S., *Phys. Rev. Lett.* **55,** 1583 (1985).
7. Rieder, K. H., and Stocker, W., *Phys. Rev. Lett.* **57,** 2548 (1986).
8. Baddorf, A. P., Lyo, I. W., Plummer, E. W., and Davis, H. L., *J. Vac. Sci. Technol. A* **5,** 782 (1987).
9. Jacobsen, K. W., and Norskov, J. K., *Phys. Rev. Lett.* **59,** 2764 (1987).
10. Astaldi, C., Bianco, A., Modesti, S., and Tosatti, E., *Phys. Rev. Lett.* **68,** 90 (1992).
11. Hayden, B. E., Lackey, D., and Schott, J., *Surg. Sci.* **239,** 119 (1990).
12. Alexander, C. S., and Pritchard, J., *J. Chem. Soc. Faraday Trans. 1* **68,** 202 (1972).
13. Shield, L. S., and Russell, W. W., *J. Phys. Chem.* **64,** 1592 (1960).
14. Beebe, R. A., Low, G. W., Jr., Wildner, E. L., and Goldwasser, S., *J. Am. Chem. Soc.* **57,** 2527 (1935).
15. Pritchard, J., and Tompkins, F. C., *J. Chem. Soc. Faraday Trans.* **56,** 540 (1960).
16. Bradley, T. L., and Stickney, R. E., *Surf. Sci.* **38,** 313 (1973).
17. Balooch, M., and Stickney, R. E., *Surf. Sci.* **44,** 310 (1974).
18. Balooch, M., Cardillo, M. J., Miller, D. R., and Stickney, R. E., *Surf. Sci.* **46,** 358 (1974).
19. Rettner, C. T., Auerbach D. J., and Michelson, H. A., *Phys. Rev. Lett.* **68,** 1164 (1992).
20. Campbell, J. M., and Campbell, C. T., *Surf. Sci.* **259,** 1 (1991).
21. Anger, G., Winkler, A., and Rendulic, K. D., *Surf. Sci.* **220,** 1 (1989).
22. Hayden, B. E., and Lamont, C. L. A., *Phys. Rev. Lett.* **63,** 1823 (1989).
23. Rasmussen, P. B., Holmblad, P. M., Taylor, P. A., and Chorkendorff, I., *Surf. Sci.* **287/288,** 79 (1993).
24. Pritchard, J., Catterick, T., and Gupta, G. K., *Surf. Sci.* **53,** 1 (1975).
25. Woodruff, D. P., Hayden, B. E., Prince, K., and Bradshaw, A. M., *Surf. Sci.* **123,** 397 (1982).
26. Truong, C. M., Rodriguez, J. A., and Goodman, D. W., *Surf. Sci. Lett.* **271,** L385 (1992).
27. Horn, K., Hussain, M., and Pritchard, J., *Surf. Sci.* **63,** 244 (1977).
28. Pritchard, J., *Surf. Sci.* **79,** 231 (1979).
29. de Jong, K. P., Geus, J. W., and Joziasse, J., *Appl. Surf. Sci.*, 273 (1980).
30. Roberts, D. L., and Griffin, G. L., *J. Catal.* **110,** 117 (1988).
31. Kohler, M. A., Cant, N. W., Wainwright, M. S., and Trimm, D. L., *J. Catal.* **117,** 188 (1989).
32. Millar, G. J., Rochester, C. H., and Waugh, K. C., *J. Chem. Soc. Faraday Trans.* **87,** 1467 (1991).
33. Papp, H., *Surf. Sci.* **63,** 182 (1977).
34. Andersson, S., *Surf. Sci.* **89,** 477 (1979).
35. Sexton, B. A., *Chem. Phys. Lett.* **63,** 451 (1979).
36. Wendelken, J. F., and Ulehla, M. V. K., *J. Vac. Sci. Technol.* **16,** 441 (1979).
37. Yu, K. Y., Spicer, W. E., Lindau, I., Pianetta, P., and Lin, S. F., *Surf. Sci.* **57,** 157 (1976).
38. Allyn, C. L., Gustafsson, T., and Plummer, E. W., *Solid State Commun.* **24,** 531 (1977).
39. Cox, D. F., and Schulz, K. H., *Surf. Sci.* **249,** 138 (1991).
40. Harendt, C., Goschnick, J., and Hirschwald, W., *Surf. Sci.* **152,** 453 (1985).
41. Tracy, J. C., *J. Chem. Phys.* **56,** 2748 (1972).
42. Kessler, J., and Thieme, F., *Surf. Sci.* **67,** 405 (1977).
43. Pritchard, J., *J. Chem. Soc. Faraday Trans.* **59,** 437 (1963).
44. Netzer, F. P., Wille, R. A., and Matthew, J. A. D., *Solid State Commun.* **21,** 97 (1977).
45. Spitzer, A., and Luth, H., *Surf. Sci.* **102,** 29 (1981).
46. Hermann, K., Bagus, P. S., and Constance, J. N., *Phys. Rev. B* **35,** 9467 (1987).
47. Bagus, P. S., Bauschlicher, C. W., and Nelin, C. J., *J. Vac. Sci. Technol. A* **2,** 905 (1984).
48. Fu, S. S., and Somorjai, G. A., *Surf. Sci.* **262,** 68 (1992).

49. Rodriguez, J. A., Clendening, W. D., and Campbell, C. T., *J. Phys. Chem.* **93,** 5238 (1989).
50. Rasmussen, P. B., Taylor, P. A., and Chorkendorff, I., *Surf. Sci.* **269/270,** 352 (1992).
51. Hadden, R. A., Vandervell, H. D., Waugh, K. C., and Webb, G., *Catal. Lett.* **1,** 27 (1988).
52. Clarke, D. B., Suzuki, I., and Bell, A. T., *J. Catal.*, **142,** 27 (1993).
53. Millar, G. M., Rochester, C. H., Howe, C., and Waugh, K. C., *Mol. Phys.* **76,** 833 (1991).
54. Rodriguez, J. A., *Langmuir* **4,** 1006 (1988).
55. Copperthwaite, R. G., Davies, P. R., Morris, M. A., Roberts, M. W., and Ryder, R. A., *Catal. Lett.* **1,** 11 (1988).
56. Nakamura, J., Rodriguez, J. A., and Campbell, C. T., *J. Condensed Matter*, in press.
57. Kohler, M. A., Lee, J. C., Trimm, D. L., Cant, N. W., and Wainwright, M. S., *Appl. Catal.* **31,** 309 (1987).
58. Chinchen, G. C., Hay, C. M., Vandervell, H. D., and Waugh, K. C., *J. Catal.* **103,** 79 (1987).
59. Evans, J. W., Wainwright, M. S., Bridgewater, A. J., and Young, D. J., *Appl. Catal.* **7,** 75 (1983).
60. Chin, A. A., Masters thesis, University of California, Berkeley, 1982.
61. Falconer, J. L., and Madix, R. J., *J. Catal.* **48,** 262 (1977).
62. Falconer, J. L., and Schwarz, J. A., *Catal. Rev.* **87,** 1100 (1983).
63. Gregory, A. R., Gelb, A., and Sibley, R., *Surf. Sci.* **74,** 497 (1978).
64. Cvetanovic, R. J., and Amenomiya, Y., *in* "Advances in Catalysis" (D. D. Eley, H. Pines, and P. B. Weisz, Eds.), Vol. 17, Academic Press, New York, 1967.
65. Kovalinka, J. A., Scholten, J. J. F., and Rasser, J. C., *J. Catal.* **48,** 365 (1977).
66. Jones, D. M., and Griffin, G. L., *J. Catal.* **80,** 40 (1983).
67. Sandoval, M. J., Master's thesis, University of California, Berkeley, 1993.
68. Chesters, M. A., Pritchard, J., and Sims, M. L., *in* "Adsorption–Desorption Phenomena" (F. Ricca, Ed.). Academic Press, London, 1972.
69. Papp, H., and Pritchard, J., *Surf. Sci.* **53,** 371 (1975).
70. Shustorovich, E., *Surf. Sci. Rep.* **6,** 1 (1986).
71. Lombardo, S., and Bell, A. T., *Surf. Sci.* **224,** 451 (1989).
72. Trapnell, B. M. W., *Proc. R. Soc. London Ser. A* **218,** 566 (1953).